Automated Computer-Controlled Tuning of Waveguide Filters Using Adaptive Network Models

Peter Harscher, *Member, IEEE,* and Rüdiger Vahldieck, *Fellow, IEEE*

***Abstract*—This paper describes a method for computer-controlled tuning of waveguide filters. The tuning algorithm is based on approximate filter network models, which take into account the effects of input/output coupling. Based on measurements of an initial filter design, the approximate network model is then corrected by optimizing the element values such that they minimize the mean square error between the measured and simulated response. The sensitivities of the tuning screws are determined directly from the sensitivities of the element values. Filter tuning is accomplished by gradient optimization of the corrected computer model rather than its physical realization. Only as a final step are the tuning screws of the physical model turned to the position determined by the optimization process.**

***Index Terms*—CAD, gradient methods, manufacturing automation, modeling, optimization methods, parameter estimation, tunable filters, waveguide filters.**

I. Introduction

THE explosive growth of satellite and terrestrial communication systems has significantly increased the market for microwave and millimeter-wave filters. To satisfy the high demand for short-term availability of filters at different mid-band frequencies, bandwidth, skirt selectivity, etc., a suitable set of standard filters is the key to fast production. In addition, these filters must be tunable and their tuning process must be automated to minimize labor cost. Depending on the filter topology, the basic three tuning techniques are: 1) mechanically; 2) magnetically; and 3) electronically.

This paper deals with mechanical tuning of filters, although the routine presented in the following is also applicable to other tuning methods. Mechanical filter tuning is generally done by hand. This process is costly, time consuming, and needs skilled operators. Generally, the expenses are directly proportional to the sensitivity of the filter elements and increase with the number of resonators or when cross couplings are used or in the case of dual-mode filters. To bypass these problems and to cut labor costs significantly, an automatic computer-controlled tuning system is introduced that offers the following features:

- only little user interaction needed;
- no accurate filter model required;
- generally applicable as long as an approximate filter model is available;
- no database or expert system necessary;
- only a few measurements are needed.

Manuscript received February 28, 2001.

The authors are with the Laboratory for Electromagnetic Fields and Microwave Electronics, Swiss Federal Institute of Technology, CH-8092 Zürich, Switzerland.

Publisher Item Identifier S 0018-9480(01)09385-1.

The key element of the automatic tuning procedure is the availability of an approximate network model of the filter structure to be tuned. The network model need only be as accurate as to provide a reliable prediction in which direction the tuning screws (with corresponding penetration depths) must be turned to increase or decrease the values of the corresponding network elements. This prediction must be valid within the tuning range of the filter. A standard network model of a direct-coupled filter has been used here. The tuning process is essentially a four-step procedure. First, the physical filter model is measured with the tuning screw position set to an initial position. For the tuning system to work, the resulting measured response must resemble that of a filter. The element values of the network model are then computed such that the model response is fitted to the measurements. This is achieved by means of a gradient optimization procedure, which minimizes the mean square error between the response of the approximate model (for which the element values are obtained from synthesis techniques or empirical values) and the measured response. The so-found element values represent the corrected network model (the true model) of the physical filter realization including all manufacturing imperfections. The second step in the tuning procedure is to determine the element sensitivities and that of the tuning screws, respectively. This requires as many measurements as there are tuning screws and provides information on how many screw turns are necessary to change the element values a prescribed amount. The third step is to optimize the corrected network model to satisfy the filter specifications. This takes place on the computer and requires only a few optimization steps, depending on the number of variables involved and the optimization strategy. The fourth step is then to turn the tuning screws to the position determined by the optimization process. In case the initial filter response and the final filter specs are too far apart, the entire process may be repeated.

It should be noted that the above procedure essentially replaces a full-wave electromagnetic modeling of the structure. This is an interesting option because correcting element values for an otherwise approximate network model and then optimizing the corrected network to specifications may be a much faster process (especially for complicated filter structures) than full-wave modeling/optimization of the entire filter structure. Furthermore, the added advantage is that the effects of manufacturing tolerances (frequently not known) are already included in this procedure.

In the literature, several attempts of automatic filter tuning techniques have been proposed, but they are either not applicable to waveguide filters or they are not as efficient as the

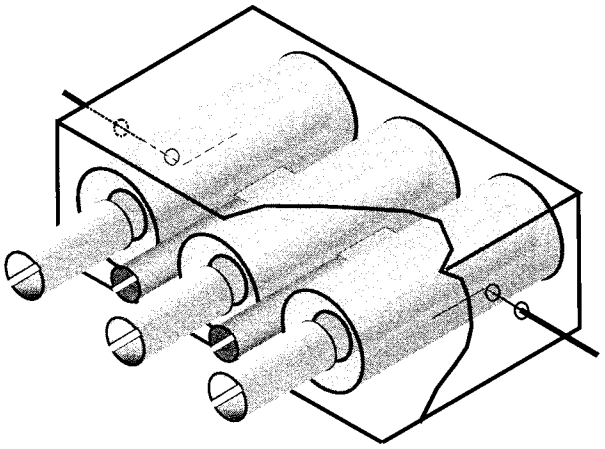

Fig. 1. Reentrant resonator filter.

above procedure. In [1], filter tuning in the time domain is described. However, this method requires a perfectly tuned filter as a template. The tuning of duplicates of this filter is then performed by a skilled operator. Reference [2] describes a lumped-model generation to characterize millimeter-wave passive components from curve fitting of measured data. This data is then used to calculate metal–insulator–metal (MIM) capacitors, interdigital capacitors, and spiral inductors using a least-squares fitting scheme. However, this scheme requires design equations of individual components. In [3], a machine learning approach for filter tuning using pattern recognition and adaptive signal-processing techniques is investigated. An unskilled human operator is still required to perform the actual tuning of the filters. References [4] and [5] introduce computer-aided tuning of *LC* filters. In both [4] and [5], low-frequency *LC* networks are used whose parameters are extracted from measurements using Monte Carlo techniques [4] and stochastic methods [5], respectively, and are, thus, very slow. In [6], pattern-search techniques in conjunction with lossless networks are employed to build up a computer-aided tuning system for determining inter-cavity couplings and resonator de-tunings of the short-circuited network under test. The problem with this method is that each cavity has to have a probe input and output during the tuning process and, therefore, cables must be changed.

In the present approach, the disadvantages of all the aforementioned techniques are avoided. To demonstrate this new automated tuning technique, we have chosen a simple three–resonator coaxial reentrant filter, as shown in Fig. 1.

For demonstration purposes only, five tuning screws are involved that are turned by precision position stepper motors. The resonant frequency of the resonators and the openings of the coupling slots can be changed with tuning screws. The filter has a Chebyshev bandpass characteristic and can be tuned over a range $f = 1.35 - 1.65$ GHz.

II. Tuning Procedure

The block diagram of Fig. 2 illustrates the automatic tuning concept steps as follows.

Step 1) Choose the desired filter specifications.
Step 2) Pre-tune the filter within the tuning range.

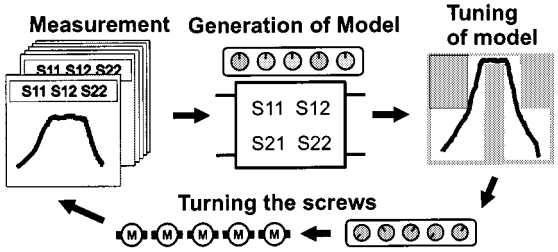

Fig. 2. Block diagram of the automatic tuning system.

Step 3) Measure S-parameters for this start (basis) position of the tuning screws.
Step 4) Extract correct element values for this basis position.
Step 5) Measure S-parameters with one screw turned at a time.
Step 6) Extract network element sensitivities.
Step 7) Tune corrected computer model to fit frequency specifications (gradient optimization).
Step 8) Turn screws according to results of Step 7).
Step 9) Repeat procedure if accuracy is not sufficient.

In the following, these steps are illustrated. To begin with, an ideal filter is synthesized according to the desired filter specifications (center frequency, ripple, and bandwidth). A three-pole Chebyshev prototype characteristic is shown in Fig. 3(a) (solid curve). The physical filter realization is roughly pre-tuned to a start (basis) position [see step 2)]. Two conditions must be satisfied: the basis position of the tuning screws must be within the tuning range of the process, and the initial filter response (screw positions d_1, d_2, d_3, d_4, d_5) must "resemble" that of a bandpass filter. The $d_i's$ are determined in a preproduction process, e.g., with respect to a defined reference position. In this basis position, S_{11}, S_{22}, and S_{21} are measured [step 3), dashed and dotted curves in Fig. 3(a)] and compared to the model response. In case of a discrepancy, the model element values must be corrected to represent the actual values imposed by the current position of the tuning screws. To extract the actual element values from the measurement, a gradient-based optimization procedure is employed in which the model response is fitted to the measured response. For that purpose, the following cost function is minimized [see step 4)]:

$$F = \sum_{\text{freq.}} \sum_{i=1}^{2} \sum_{j=1}^{2} \Big(abs\big(S_{ij}^{\text{model}}\big) - abs\big(S_{ij}^{\text{measured}}\big) \Big)^2. \quad (1)$$

Fig. 3(b) shows the response of the network model (dashed lines), calculated with parameter values determined by the above parameter-extraction process. The curves fit almost perfectly to the measured (solid lines) filter response.

Subsequently [see step 5)], five additional measurements are performed turning each screw at a time (i.e., first measurement: $d_1 + \Delta d, d_2, d_3, d_4, d_5$) to determine the sensitivities of the element values and to establish a relationship between the element value and the corresponding screw depth (turns) as follows:

$$\text{Element\_value}_i = \text{Element\_value}_i(\text{basis position}) + \sum_{j=1}^{5} \text{sensitivity}_{j,i} \frac{\Delta d_j}{d_j}. \quad (2)$$

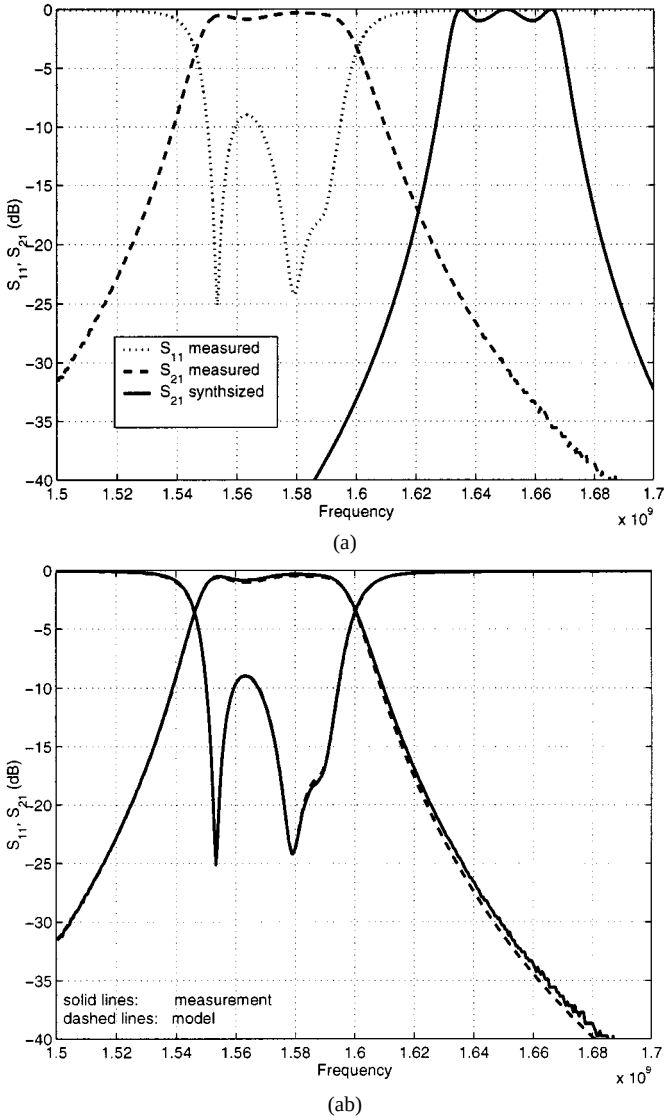

Fig. 3. (a) Initial response. (b) After parameter extraction.

For this purpose, after each measurement, the elements for the equivalent-circuit model are extracted similar to step 4). Comparing the five parameter sets with the parameter values of the basis position and using the known screw positions for all sets of measurements, the network sensitivities can be calculated.

A comparison between the ideal element values (filter synthesis) and the extracted values at basis position of the tuning screws provide an indication as to which screw must be turned to achieve a certain effect.

In step 7), the model parameters of the measured filter are optimized starting with the element values at basis position. The target values are the prototype values. This is another gradient optimization process since the individual parameters (elements) are also influenced by neighboring screws. This effect is included in (2). As a result, the optimal screw positions are obtained.

Finally, a test measurement is made. If the accuracy is not sufficient, the procedure must be repeated.

III. Network Models

The network model chosen for the modeling of the filter structure under test is very important for the success of the automated tuning process. In this study, two different network models have been investigated. While the lumped-element model does not include tuning elements of the input/output coupling, the transmission-line model does.

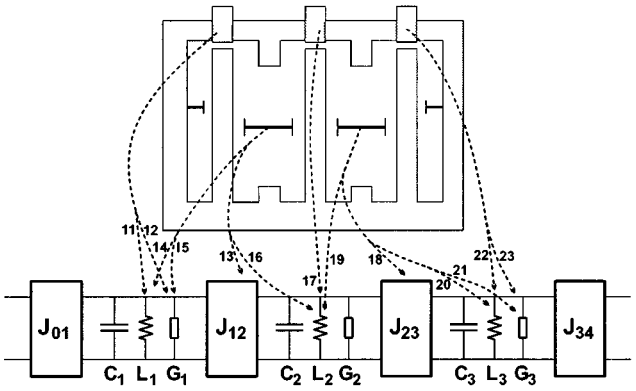

Fig. 4. Theoretical model and relation between tuning screws and elements of the model.

A. Lumped LCR-Parallel Resonant Circuit Coupled With Admittance Inverters (Model 1)

The first model used for the automatic tuning system is shown in Fig. 4. It consists of capacitors, inductors, resistors, and admittance inverters and is derived from a prototype network of direct-coupled filters (e.g., [7]).

The resonators are represented by parallel resonant circuits and the coupling sections are described by admittance inverters. To take losses into account, resistors are introduced. Parameter extraction is achieved through a gradient-based optimization process, where the modeled filter characteristics are fitted to the measured filter S-parameters (target functions) with the element values of the model as variables. Those values are changed until sufficient accuracy between model and measurement is reached. Fig. 4 shows the real filter layout and the corresponding network elements. The inductances and capacitances of the parallel resonant circuits are related to each other through the resonant frequencies. To minimize the number of parameters for the optimization, the capacitance values are fixed. This is necessary to obtain uniqueness of the model [8].

To calculate the scattering parameters of the model, the resonant circuits and the coupling elements are transformed into $ABCD$ matrices

$$[ADCD] = \begin{vmatrix} 1 & 0 \\ Y_i(s) & 1 \end{vmatrix} \quad [ABCD] = \begin{vmatrix} 0 & \frac{1}{J_i(s)} \\ -J_i(s) & 0 \end{vmatrix} \tag{3}$$

which are normalized with respect to frequency. Y is the admittance of a resonant circuit and $s = j\omega$. The overall $ABCD$ matrix of the entire filter model is then a product of the individual filter sections. This matrix is then transformed to the admittance matrix (Y) and subsequently into the scattering parameter matrix (S). This algorithm is approximately 20 times faster than direct calculation of the *RLC* network.

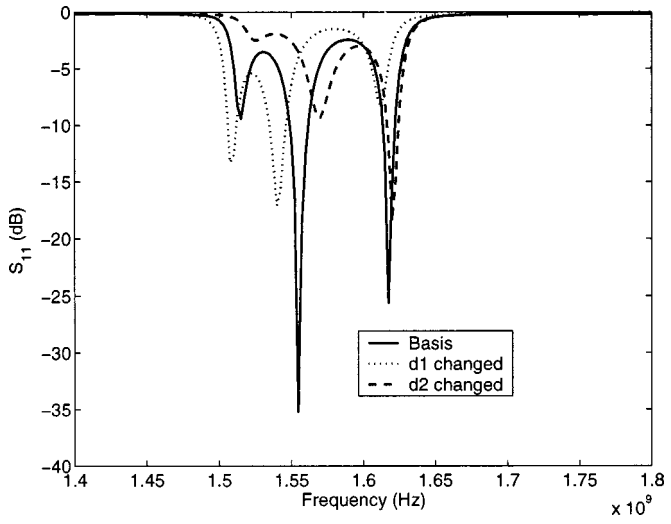

Fig. 5. Measurement of S_{11}.

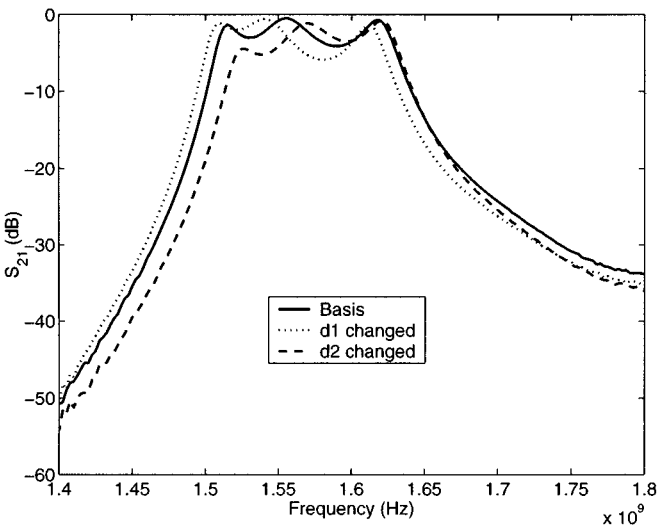

Fig. 6. Measurement of S_{21}.

The correlation between measured S-parameters, parameter values, and network sensitivities is shown in the following matrix relationship:

$$\begin{bmatrix} S_{11} & S_{22} & S_{21} \\ \frac{\partial S_{11}}{\partial d_1} & \frac{\partial S_{22}}{\partial d_1} & \frac{\partial S_{21}}{\partial d_1} \\ \frac{\partial S_{11}}{\partial d_2} & \frac{\partial S_{22}}{\partial d_2} & \frac{\partial S_{21}}{\partial d_2} \\ \frac{\partial S_{11}}{\partial d_3} & \frac{\partial S_{22}}{\partial d_3} & \frac{\partial S_{21}}{\partial d_3} \\ \frac{\partial S_{11}}{\partial d_4} & \frac{\partial S_{22}}{\partial d_4} & \frac{\partial S_{21}}{\partial d_4} \\ \frac{\partial S_{11}}{\partial d_5} & \frac{\partial S_{22}}{\partial d_5} & \frac{\partial S_{21}}{\partial d_5} \end{bmatrix}$$

$$\rightarrow \begin{matrix} J_{12} & J_{23} & L_1 & L_2 & L_3 & G_1 & G_2 & G_3 \\ 0 & 0 & \frac{\partial L_1}{\partial d_1} & 0 & 0 & \frac{\partial G_1}{\partial d_1} & 0 & 0 \\ \frac{\partial J_{12}}{\partial d_2} & 0 & \frac{\partial L_1}{\partial d_2} & \frac{\partial L_2}{\partial d_2} & 0 & \frac{\partial G_1}{\partial d_2} & 0 & 0 \\ 0 & 0 & 0 & \frac{\partial L_2}{\partial d_3} & 0 & 0 & 0 & 0 \\ 0 & \frac{\partial J_{23}}{\partial d_4} & 0 & \frac{\partial L_2}{\partial d_4} & \frac{\partial L_3}{\partial d_4} & 0 & 0 & \frac{\partial G_3}{\partial d_4} \\ 0 & 0 & 0 & 0 & \frac{\partial L_3}{\partial d_5} & 0 & 0 & \frac{\partial G_3}{\partial d_5} \end{matrix} \quad (4)$$

From here, it is obvious that each screw affects not only the element value it is supposed to, but also the network elements nearby. The influence of the screws on the network elements are found from a sensitivity analysis. The zeros in matrix (4) represent low sensitivities that can be neglected. For example, screw 1 mainly effects L_1 and G_1 [second row in matrix (4)].

The penetration depths of d_i are measured with respect to a defined reference position. In this basis position, S_{11}, S_{22}, and S_{21} are measured (step 3). The results for S_{11} and S_{21}, respectively, are shown in Figs. 5 and 6 (solid lines). Subsequently [see step 5)], five additional measurements are performed turning each screw at a time. This provides again five data sets for S_{11}, S_{22}, and S_{21}, which are all given in Table I. As an example, Figs. 5 and 6 show the measured results after turning screw 1 or screw 2.

TABLE I
MEASUREMENTS FOR CORRECTING THE THEORETICAL FILTER MODEL

	$\mathbf{d_1}$ [mm]	$\mathbf{d_2}$ [mm]	$\mathbf{d_3}$ [mm]	$\mathbf{d_4}$ [mm]	$\mathbf{d_5}$ [mm]
Basis	1.61	9.73	1.05	9.73	1.61
Variat					
1	**1.16**	9.73	1.05	9.73	1.61
2	1.61	**6.73**	1.05	9.73	1.61
3	1.61	9.73	**0.85**	9.73	1.61
4	1.61	9.73	1.05	**6.73**	1.61
5	1.61	9.73	1.05	9.73	**1.16**

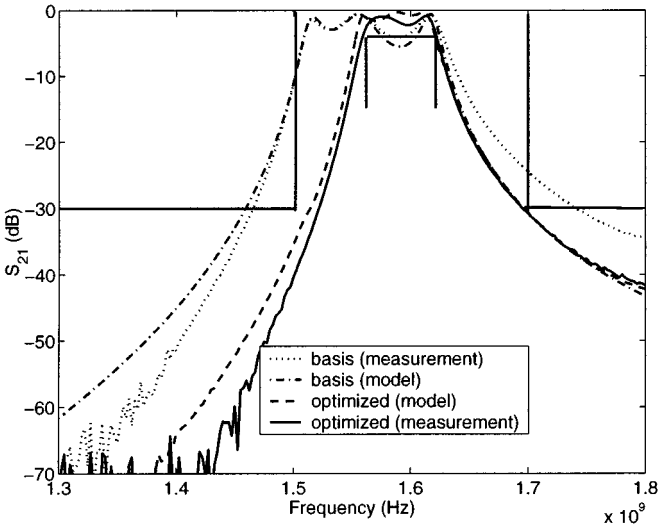

Fig. 7. Basis position and optimized filter; center frequency and bandwidth changed.

Following the tuning procedure described in the previous paragraph, the filter was tuned to the desired response, which is shown in Fig. 7. It shows the corrected model prediction in comparison with the basis position of the filter screws. In the same figure, the corrected and optimized model as well as the corresponding measured response is also shown. The bandwidth of the original filter at the basis position was about 100 MHz with a 40-MHz offset from the desired response.

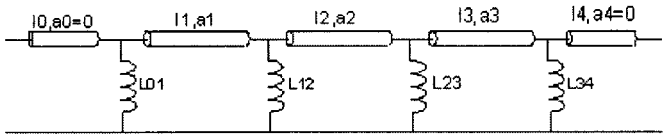

Fig. 8. Transmission-line model.

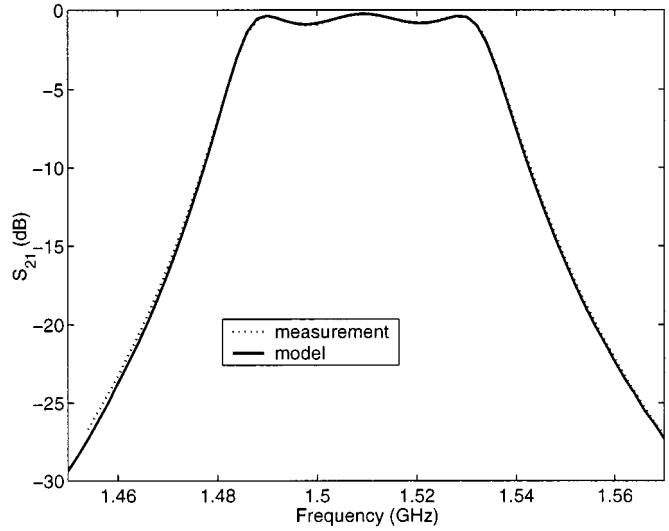

(a)

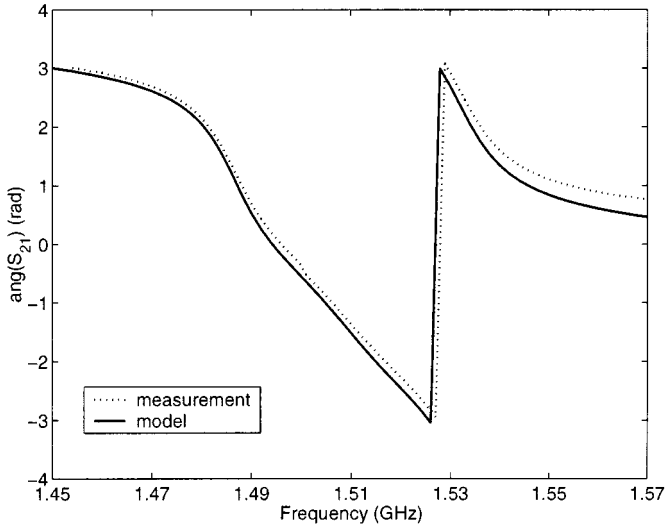

(b)

Fig. 9. Modeled and measured S_{21}. (a) Magnitude. (b) Phase.

After 250 optimization steps, the bandwidth was reduced to 50 MHz and was shifted to within the desired filter window. The whole process took approximately 5 min (measurements, calculation, and stepper motor positioning), whereby most of the time was consumed by the data-acquisition process.

B. Inductively Coupled $\lambda/2$ Transmission Lines (Model 2)

The second model used in our investigation was based on $\lambda/2$ transmission-line sections coupled by parallel inductances, as shown in Fig. 8.

Here also, the parameter values for an ideal filter can be obtained by filter synthesis. To simulate the real filter with this transmission-line model, the parameter values are again extracted from measured S-parameters. The procedure is the same as described for the lumped-element model of the previous paragraph. The resonant frequencies of the resonators are modeled by defined transmission-line lengths l_1, l_2, and l_3 and the losses by attenuation constants a_1, a_2, and a_3. The couplings between the resonators are modeled by the inductances L_{12}, L_{23}, and L_{34}. Additionally, this model takes into account effects of the input and output coupling probes L_{01} and L_{34}, which cause a phase shift in the overall S-parameters. Although this measure is only a crude approximation of the coupling probe effects, it is sufficient to model its main impact [9]. If the complete model of the coupling probes as described in [9] is used, the model is no longer unique [8] and the parameter-extraction process can give ambiguous parameter sets for one and the same measured filter characteristics.

With the model in Fig. 8, it is easily possible to also model the phase of the S-parameters. The cost function is then used for the gradient-based parameter extraction, shown in (5), at the top of the following page.

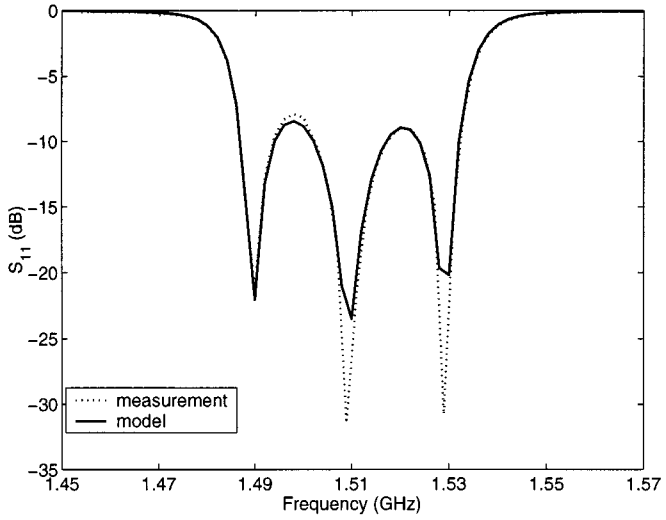

(a)

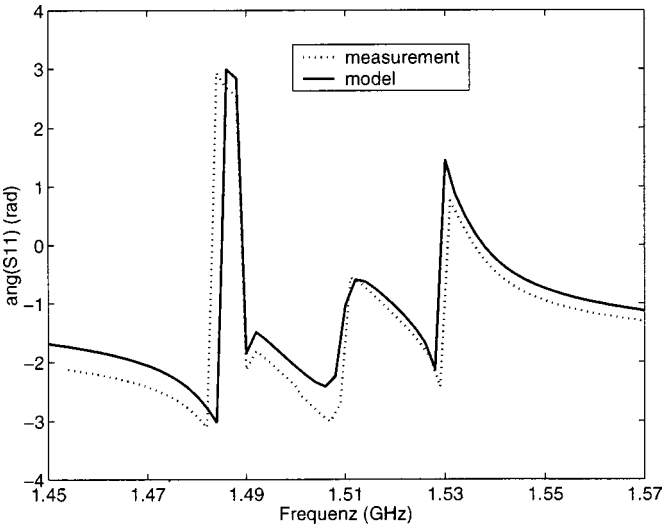

(b)

Fig. 10. Modeled and measured S_{11}. (a) Magnitude. (b) Phase.

$$F = \sum_{freq.} \sum_{i=1}^{2} \sum_{j=1}^{2} \left[\left(\text{real}(S_{ij}^{\text{computed}}) - \text{real}(S_{ij}^{\text{measured}}) \right)^2 + \left(\text{imag}(S_{ij}^{\text{computed}}) - \text{imag}(S_{ij}^{\text{measured}}) \right)^2 \right] \quad (5)$$

Using the phase of the S-parameters leads to much faster convergence of the optimization process and much greater accuracy of the element values. This is demonstrated in Figs. 9 and 10.

Compared to the *LCR* model, the resonant frequencies of the resonators are modeled by only one parameter (line length) rather than by two (parallel *L*-*C* with *C* fixed). Due to the periodicity of transmission lines (waveguide sections), this measure represents the frequency-dependent behavior of waveguide filters more realistically (compare Figs. 9(a) and 7). Since the effects of the input and output coupling probes are also included in the transmission-line model, the measured S-parameters can be modeled in the complex plane. Thus, the chance of finding ambiguous solutions in the parameter-extraction process is drastically reduced compared to the approach where only absolute values of the S-parameters are used.

IV. Conclusions

An automatic tuning system for waveguide filters based on approximate network models has been introduced. The exact element values are extracted from measured scattering parameters of the physical filter structure by a gradient optimization procedure. It was shown that the accuracy of the approximate network model chosen to describe the filter is very important for the feasibility of the approach. The tuning system was demonstrated by using a three-pole reentrant resonator filter with a tuning range of 1.35–1.65 GHz. It was shown that within a frequency offset of ± 50 MHz, the automatic tuning procedure works very well.

References

[1] "Simplified filter tuning using time domain," Hewlett-Packard, , Santa Rosa, CA, HP Applicat. Note 1287–8, 1999.

[2] N. Kinayman and N. Jain, "Automatic and accurate lumped-model generation of millimeter wave passive components using EM simulator," in *Proc. 29th European Microwave Conf.*, vol. 1, 1999, pp. 170–173.

[3] A. R. Mirzai, "Intelligent alignment of waveguide filters using a machine learning approach," *IEEE Trans. Microwave Theory Tech.*, vol. 37, pp. 166–173, Jan. 1989.

[4] J. F. Pinel, "Computer-aided network tuning," *IEEE Trans. Circuit Theory*, vol. CT–18, pp. 192–194, Jan. 1971.

[5] Yu Jiliang and J. K. Fidler, "An automatic LC filter tuning system by optimization," in *Proc. 3rd IEEE Int. Electron., Circuits, Syst. Conf.*, vol. 1, 1996, pp. 215–218.

[6] L. Accatino, "Computer-aided tuning of microwave filters," CSELT, Turin, Italy, Tech. Rep. XV 3, 1987.

[7] G. Matthaei, L. Young, and E. M. T. Jones, "Microwave filters," in *Impedance-Matching Networks and Coupling Structures* Artech House, Norwood, MA, 1980.

[8] M. H. Bakr, J. W. Bandler, and N. Georgieva, "An aggressive approach to parameter extraction," *IEEE Trans. Microwave Theory Tech.*, vol. 47, pp. 2528–2539, Dec. 1999.

[9] D. Kaifez, "Q-factor measurement techniques," *R. F. Des.*, pp. 56–73, Aug. 1999.

Peter Harscher (M'97) received the Diploma Engineer degree in telecommunications from the Rheinisch-Westphälische Technische Hochschule Aachen, Aachen, Germany, in March 1997, and is currently working toward the Ph.D. degree in electromagnetic fields and microwave electronics at the Swiss Federal Institute of Technology, Zurich, Switzerland.

During the summer of 1997, he was a Design Engineer in the Airborn, Ground, and Naval Systems Division, Daimler Benz Aerospace, Ulm, Germany. In November 1997, he joined the Laboratory for Electromagnetic Fields and Microwave Electronics, Swiss Federal Institute of Technology. He is currently involved in computer-aided design (CAD) of microwave circuits using numerical methods, like the finite-element method, and in the development of an automatic computer-controlled tuning system for microwave filters.

Rüdiger Vahldieck (M'85–SM'86–F'99) received the Dipl.-Ing. and Dr.-Ing. degrees in electrical engineering from the University of Bremen, Bremen, Germany, in 1980 and 1983, respectively.

From 1984 to 1986, he was a Research Associate at the University of Ottawa, Ottawa, ON, Canada. In 1986, he joined the Department of Electrical and Computer Engineering, University of Victoria, Victoria, BC, Canada, where he became a Full Professor in 1991. During the fall and spring of 1992-1993, he was a Visiting Scientist at the Ferdinand-Braun-Institute für Hochfrequenztechnik, Berlin, Germany. Since 1997, he has been a Professor of electromagnetic-field theory at the Swiss Federal Institute of Technology, Zurich, Switzerland. Since 1981 he has authored or co–authored over 200 technical papers in books, journals, and conferences, mainly in the field of microwave CAD. His research interests include numerical methods to model electromagnetic fields in the general area of electromagnetic compatibility (EMC), particularly for CAD of microwave, millimeter-wave, and optoelectronic integrated circuits.

Prof. Vahldieck is the past-president of the IEEE 2000 International Zurich Seminar on Broadband Communications (IZS'2000) and president of the EMC Congress, Zurich, Switzerland. Since 1992, he has served on the Technical Program Committee of the IEEE Microwave Theory and Techniques Society (IEEE MTT-S) International Microwave Symposium, the IEEE MTT-S Technical Committee on Microwave Field Theory and, in 1999, on the Technical Program Committee of the European Microwave Conference. He is the chairman of the Swiss Joint Chapters of the IEEE MTT-S, IEEE Antennas and Propagation Society (IEEE AP-S), and the IEEE Electromagnetics Compatibility Society (IEEE EMC-S). He is an associate editor for the IEEE Microwave and Wireless Components Letters and a member of the Editorial Board for the IEEE Transactions on Microwave Theory and Techniques. He was a corecipient of the 1983 Outstanding Publication Award of the Institution of Electronic and Radio Engineers. He was also the recipient of the 1996 J. K. Mitra Award of the Institute of Electronics and Telecommunications Engineers (IETE) for the Best Research Paper of 1995.